HHS Public Access

Author manuscript

J Immunol. Author manuscript; available in PMC 2016 March 23.

Published in final edited form as:

J Immunol. 2013 December 15; 191(12): 5993–6001. doi:10.4049/jimmunol.1203541.

Batf3 and *Id2* Have a Synergistic Effect on *Irf8*-Directed Classical CD8α$^+$ Dendritic Cell Development

Hemant Jaiswal[*], **Monika Kaushik**[*], **Rachid Sougrat**[†], **Monica Gupta**[‡], **Anup Dey**[‡], **Rohit Verma**[*], **Keiko Ozato**[‡], and **Prafullakumar Tailor**[*]

[*]Laboratory of Innate Immunity, National Institute of Immunology, New Delhi 110067, India

[†]Nanobiology Lab, King Abdullah University of Science and Technology, Thuwal 23955-6900, Saudi Arabia

[‡]Laboratory of Molecular Growth Regulation, National Institute of Child Health and Human Development, National Institutes of Health, Bethesda, MD 20892

Abstract

Dendritic cells (DCs) are heterogeneous cell populations represented by different subtypes, each varying in terms of gene expression patterns and specific functions. Recent studies identified transcription factors essential for the development of different DC subtypes, yet molecular mechanisms for the developmental program and functions remain poorly understood. In this study, we developed and characterized a mouse DC progenitor-like cell line, designated DC9, from *Irf8*$^{-/-}$ bone marrow cells as a model for DC development and function. Expression of *Irf8* in DC9 cells led to plasmacytoid DCs and CD8α$^+$ DC–like cells, with a concomitant increase in plasmacytoid DC– and CD8α$^+$ DC–specific gene transcripts and induction of type I IFNs and IL12p40 following TLR ligand stimulation. *Irf8* expression in DC9 cells led to an increase in *Id2* and *Batf3* transcript levels, transcription factors shown to be important for the development of CD8α$^+$ DCs. We show that, without *Irf8*, expression of *Id2* and *Batf3* was not sufficient for directing classical CD8α$^+$ DC development. When coexpressed with *Irf8*, *Batf3* and *Id2* had a synergistic effect on classical CD8α$^+$ DC development. We demonstrate that *Irf8* is upstream of *Batf3* and *Id2* in the classical CD8α$^+$ DC developmental program and define the hierarchical relationship of transcription factors important for classical CD8α$^+$ DC development. *The Journal of Immunology*, 2013, 191: 5993–6001.

Dendritic cells (DCs) play a critical role at the onset of infection to control innate immune responses and facilitate initiation of appropriate adaptive immune responses. DCs are represented by different subclasses, varying in terms of characteristics, such as specific cytokine production, Ag presentation, anatomical distribution, and gene expression patterns (1, 2). DCs are primarily classified as four major subtypes: plasmacytoid DCs (pDC), CD4$^+$

Address correspondence and reprint requests to Dr. Prafullakumar Tailor, Laboratory of Innate Immunity, National Institute of Immunology, Aruna Asaf Ali Marg, New Delhi 110067, India. tailorp@nii.ac.in.

The online version of this article contains supplemental material.

Disclosures

The authors have no financial conflicts of interest.

DCs and CD8α$^+$ DCs, CD4$^-$CD8$^-$ double-negative DCs, and tissue-specific DCs (3, 4). Each DC subclass expresses a specific set of genes important for development and defined functions (5). pDCs produce very high levels of type I IFNs but have a limited capacity for Ag processing and presentation (6, 7). CD4$^+$ DCs and CD8α$^+$ DCs play a major role in Ag presentation, with CD8α$^+$ DCs having a special ability to produce very high levels of IL-12 and Ag cross-presentation. Since the discovery of a specialized type I IFN–producing pDC subclass, the origin of different DC subclasses, as well as the generation of DC diversity, has been the topic of detailed studies (6, 8). The significance of CD8α$^+$ DCs was in doubt until the recent identification of an equivalent human population by independent groups (9–13). The Lin$^-$CD11c$^-$MHCII$^-$Flt3$^+$M-CSFR$^+$c-Kit$^+$ fraction in mouse bone marrow is a common DC progenitor population that can differentiate into all major DC subsets (14–16). Flt3-L, GM-CSF, and M-CSF signaling plays a critical role in DC development and the resultant outcome of DC subclass profiles (14, 17–19). Flt3-L and M-CSF culture leads to pDCs and conventional DCs (cDCs), whereas GM-CSF–based culture preferentially induces the CD4$^+$ DC subset by blocking the development of pDCs and the CD8α$^+$ DC subset (17–20).

IRF family members play critical roles in DC development and function. Together, *Irf4* and *Irf8* govern the molecular programs regulating DC subset development and functional diversity. *Irf4* controls CD4$^+$ DC development, whereas *Irf8* is essential for CD8α$^+$ DCs and pDCs (18, 21–23). GM-CSF signaling activates Stat5, which suppresses *Irf8* gene transcription, resulting in development of only the CD4$^+$ DC subtype (20). *Irf2* blocks IFNAR signaling, and it is essential for CD4$^+$ DC development (24). *Irf1* deficiency leads to a progressive increase in pDCs and CD8α$^+$ DCs, which are tolerogenic in nature (25). Basic helix-loop-helix transcription factors *E2.2* and *Id2* are pivotal in DC development (26, 27). *E2.2* is required for pDC-specific gene expression and regulates *Irf8* transcription in pDCs (26). Interestingly, *Id2*, a member of the inhibitor class of the helix-loop-helix transcription factor family, is required for CD8α$^+$ DC development, and it inhibits pDC development, probably by blocking the action of *E2.2* (28). *Spib* and *Ikaros* transcription factors are required for pDC development, and PU.1 controls cDC development (29, 30). Recently, two major cDC subsets were described based on their surface expression of CD11b and CD103. CD103$^+$ cDCs, identified in the lymphoid organs (except the lamina propria), are like CD8$^+$ DCs and are developmentally regulated by Flt3-L, *Id2*, and *Irf8*, whereas the CD11b$^+$ cDC population is regulated by Flt3-L and M-CSFR, independent of *Id2* and *Irf8* (31). *Batf3* transcription factor is essential for CD8α$^+$ DC development and its equivalent CD103$^+$CD11b$^-$ DCs in lung, intestine, mesenteric lymph nodes, dermis, and skin-draining lymph nodes (32). A recent study (33) demonstrated that the interaction of *Batf* and *Batf2* with IRFs can compensate for the absence of *Batf3* in the presence of pathogen infection or IL-12 to guide an alternate CD8α$^+$ DC development. *Batf3* gene is regulated by *Nfil3*; hence *Batf3*-null mice and *Nfil3*-null mice lack CD8α$^+$ DCs (34). Zinc finger transcription factor zDC (*Zbtb46*) is expressed specifically in the cDC population, and expression of zDC differentiates classical DCs from pDCs and the monocyte–macrophage lineage population (35, 36). Although studies with knockout mouse models led to the identification of a set of transcription factors critical for DC development, the contribution of each transcription factor and cross-talk between these factors have not been fully explored (1, 4). A major hurdle in studying DC biology has been the limitation of the number of DCs available for

experiments, either ex vivo from mice tissues or in vitro from bone marrow cultures that have a short lifespan. Moreover, few, if any, characterized cell lines are suitable for DC development and functional studies.

In the current study, we developed a Flt3-L–dependent DC line from *Irf8*-null mice as a model to study DC development. We show that *Irf8* is upstream of *Id2* and *Batf3* transcription factors. Expression of *Irf8* in DC9 cells led to an increase in *Batf3*, but not *Batf* or *Batf2*, transcript levels. Expression of *Id2* and *Batf3* is not sufficient and *Irf8* is required for the development of classical CD8α$^+$ DCs. *Id2* and *Batf3*, when coexpressed, showed synergy with *Irf8* to promote classical CD8α$^+$ DC development. Together, this study illustrates that *Irf8* plays a central role in the development of classical CD8α$^+$ DCs.

Materials and Methods

Mice and cell cultures

All animal work conformed to the guidelines of institute animal ethics committee at National Institute of Immunology and the animal care and use committee at the National Institute of Child Health and Human Development. Bone marrow mononuclear cells were cultured in the presence of Flt3-L (100 ng/ml; PeproTech) to generate DCs (18, 37, 38). For developing a cell line, mouse bone marrow culture medium was replenished as required. Bone marrow–derived DC (BMDC) culture showing good growth was frozen and thawed several times. Cell morphology was monitored by Giemsa staining of cytospin preparations. DC surface markers were examined by flow cytometry using anti-CD11c, anti-CD11b, anti-B220, anti-CD8α, and anti–I-A^b Abs (BD Pharmingen) and biotin labeled anti-SiglecH Ab (Hycult Biotechnology), anti-CD115, anti-CD127, anti-CD172a and purified anti-F4/80 Ab (e-Bioscience). For detection of CD135, cells were cultured in the absence of Flt3-L for 12 h and stained with anti-CD135 Ab (eBioscience). Data were analyzed using FlowJo software (Tree Star, San Carlos, CA). For stimulation with TLR ligands, cells were treated with 1 μg/ml CpG (1826) or 1 μg/ml LPS (*Escherichia coli*) for the indicated period of time, and cells were harvested for transcript analysis by quantitative PCR or surface marker analysis by flow cytometry.

Total RNA was extracted using an RNeasy Mini kit (QIAGEN), and cDNA was prepared using Superscript II enzyme (Invitrogen), according to the manufacturers' protocol. For real-time PCR, amplification of sample cDNA was monitored with the fluorescent DNA-binding dye SYBR Green (FAST SYBR Green PCR Master Mix kit) in combination with the 7500 Fast real-time PCR System (both from Applied Biosystems), according to the manufacturer's instructions. Expression levels of *Batf* family members were also analyzed by Prime-Time assays (Integrated DNA Technology). Transcript levels were normalized to *Gapdh* levels, and samples showing undetectable transcript levels were normalized to Ct values of 35 for the calculation of fold change in gene expression. Primer sequences used for PCR are available on request.

Retroviral vectors and transduction

Murine stem cell virus (MSCV) retroviral vectors for *Irf8* and mutants were described earlier (18, 23, 37, 39). *Id2*, *Batf3*, and *Nfil3* gene cDNAs were amplified from mouse BMDCs and cloned into a MSCV-puro retroviral vector. For coexpression of *Id2*, *Batf3*, and *Irf8*, the respective genes were cloned into a MSCV retroviral vector using the internal ribosome entry sequence (IRES) of encephalomyocarditis virus from a commercially available vector. DC9 cells were transduced with viral supernatants by spinoculation (2400 rpm, 33°C, 1 h) with 4 μg/ml polybrene and selected with 2 μg/ml puromycin for 48 h, as described earlier (39). After puromycin selection, cells were harvested immediately for RNA extraction or flow cytometry analysis, unless incubated with the TLR ligands for a specified period. For confocal microscopy analysis, DC9 cells were transduced with MSCV-*Irf8*-GFP-puro and MSCV-GFP-puro retroviruses. For in vivo analysis, DC9 cells were transduced with Mig-control-IRES-hCD8t and Mig-*Irf8*-IRES-hCD8t retroviruses expressing truncated human CD8 surface marker (40). At 48 h posttransduction, equal numbers of cells were introduced into mice by retro-orbital injection. One day postinjection, spleen populations were analyzed by flow cytometry against the human $CD8\alpha^+$ population (anti-human CD8 Ab; BioLegend). To study the effect of *Irf8* on pDC- and $CD8\alpha^+$ DC–specific gene expression over 6 d of culture, DC9 cells were transduced with Mig-control-IRES-hCD8t and Mig-*Irf8*-IRES-hCD8t retroviruses, human CD8-expressing cells were purified using anti-human CD8 MicroBeads (Miltenyi Biotec) every day starting at 24 h posttransduction, and gene expression was analyzed by real-time PCR.

Confocal microscopy

Cells were fixed in 4% paraformaldehyde for 10 min and permeabilized with 100% methanol at room temperature. After blocking with 5% BSA for 30 min, cells were stained with mAb for α-tubulin, diluted at 1:2000 (Sigma) for 1 h, followed by staining with Alexa Fluor 568 anti-mouse (Molecular Probes) secondary Ab. Cells were counterstained with Hoechst 33342 (Sigma). Images were collected with a Leica SP2 AOBS inverted confocal microscope with a 63× oil-immersion objective (NA 1.32). The magnification scale was determined using Leica software.

Electron microscopy studies

DC9 cells were transduced with either MSCV control or Irf8-expressing virus and selected for 48 h using puromycin, as mentioned earlier. Cell populations were treated with CpG (1826; 1 μg/ml) for 24 h and subjected to electron microscopy studies. Cells were fixed in 2.5% glutaraldehyde and postfixed in reduced osmium (2% aqueous osmium tetroxide and 3% aqueous potassium ferrocyanide) for 1 h at room temperature. Gradual dehydration was carried in ethanol (from 70 to 100% ethanol). Cells were then embedded in epoxy resin and polymerized at 60°C for 16 h. Ultrathin sections, ranging from 70 to 90 nm, were cut using a Leica EMUC6 ultra-microtome (Leica, Germany), and collected on 200 mesh copper grids. Sections were stained with lead citrate for 2 min. The transmission electron microscopy examination was done using a Tecnai G12 Spirit BioTWIN electron microscope (FEI Company, Eindhoven, The Netherlands) operating at 120 kV. Images were recorded with a 4k*4k CCD Eagle camera (FEI Company).

Immunoblot analysis

Cells were washed with chilled PBS and lysed in RIPA buffer (50 mM Tris-HCl; pH 7.4), 150 mM NaCl, 1% Nonidet P-40, 0.5% deoxycholate, 0.1% SDS, 1 mM EGTA, 5 mM EDTA, 1 mM PMSF with cOmplete EDTA-free Protease Inhibitor Cocktail Tablets; Roche Diagnostics) on ice for 15 min. Cell lysates were clarified by centrifugation at 16,000 × g for 10 min at 4°C, and supernatant was analyzed by loading (equal cell numbers) onto 4–12% NuPAGE Bis-Tris gel (Invitrogen, Carlsbad, CA), transferred onto Hybond-LFP polyvinylidene difluoride membrane (GE Healthcare, Little Chalfont, Buckinghamshire, U.K.), and reacted with anti-ID2 Ab (rabbit polyclonal; Santa Cruz Biotechnology), anti-IRF8 Ab (goat polyclonal; Santa Cruz Biotechnology), and anti-GAPDH Ab (rabbit monoclonal; Cell Signaling Technology). Secondary detection was carried out with HRP-conjugated anti-rabbit IgG or anti-goat IgG (Santa Cruz Biotechnology), followed by chemiluminescence development with ECL Plus reagent (GE Healthcare). For detection of ERK phosphorylation, DC9 cells were cultured in RPMI 1640, without FBS and Flt3-L, for 2 h, followed by treatment with M-CSF (50 ng/ml; Prospec) for 1 h in the presence of 10% FBS, and they were processed for Western blot using anti-ERK and anti-phospho ERK Abs (cat. #9102 and cat. #4370, respectively; Cell Signaling Technology). Secondary detection was carried out with HRP-conjugated anti-rabbit IgG (Santa Cruz Biotechnology). The procedure for Western blot was the same as described above.

Results

Characterization of DC cell line

To develop a DC line, mouse bone marrow cells were cultured in the presence of Flt3-L, as described in our earlier studies (37). Although live cells could not be seen past 3 wk in the *Irf8*$^{+/+}$ cultures, one of the similar cultures from *Irf8*$^{-/-}$ mice grew continuously only in presence of Flt3-L and was established as DC9 cells. DC9 cells were maintained in culture for >4 y in the presence of Flt3-L; they have been frozen and thawed multiple times, and characterization was carried out within six or seven passages after thawing. Expression of *Irf8* by retroviral transduction led to the growth arrest of the cells (Fig. 1B). CD11c, SiglecH, and CD11b were detected by flow cytometry analysis, suggesting a DC-committed population. Expression of *Irf8* led to an increase in CD115 (M-CSFR), SiglecH, and CD11b, whereas CD127 and CD172a remained unchanged, and B220 was very low (Fig. 1C). CD135 could not be detected in ongoing cultures; removal of Flt3-L for a brief period led to efficient detection of CD135 on DC9 cells (Supplemental Fig. 1A). The monocyte–macrophage marker F4/80 was not detected on control or *Irf8*-expressing populations (Supplemental Fig. 1B). Stimulation of DC9 cells with M-CSF for a short period led to efficient phosphorylation of ERK, indicating that M-CSF– signaling components were functional in DC9 cells (41) (Supplemental Fig. 1C).

We first examined the expression of pDC and CD8α^{+} DC transcripts in *Irf8*$^{+/+}$ and *Irf8*$^{-/-}$ BMDCs. As expected, we noticed a reduction in the pDC-specific transcripts *E2.2*, Spib, Siglech, and *B220* in *Irf8*$^{-/-}$ DCs compared with *Irf8*$^{+/+}$ DCs. CD8α^{+} DC–specific genes *Id2*, *Batf3*, *Tlr11*, and *Ciita* were expressed at very low levels in *Irf8*$^{-/-}$ DCs (Fig. 1D). Expression of *Irf8* in DC9 cells led to an increase in pDC-specific gene transcripts, such as

Spib, *Siglech*, and *B220*, whereas levels of *E2.2* remained unchanged. *Irf8*-transduced cells also showed higher levels of CD8α$^+$ DC–specific genes *Id2*, *Batf3*, *Ciita*, and *Tlr11* (Fig. 1E). The increase in gene transcripts seen in DC9 cells was specific to *Irf8* expression, because the transcript levels in cells expressing mutant Irf8^{R289E} remained similar to control vector–transduced cells (Fig. 1E). *Irf8*-induced gene expression increased 40–80-fold by day 6 posttransduction (Supplemental Fig. 2A). CpG stimulation of *Irf8*-transduced DC9 cells led to a further increase in the pDC-specific transcripts of *Spib*, *Ly49Q*, *Irf7*, and *120G8* and led to the appearance of CD8α transcripts, whereas the expression level of *E2.2*, *B220*, and *Id2* was unaffected by CpG stimulation (Supplemental Fig. 2B). Correlating with our gene-expression data, we noticed that CD8α and MHC class II (MHCII) appeared on the surface of DC9 cells expressing *Irf8*^{WT}, whereas these markers were not detected in the control vector or IRF association domain mutant *Irf8*^{R289E}-expressing cells (*Irf8* mutant Arg289Glu does not form a complex with partner molecules like *Irf2* and PU.1 and fails to bind to target DNA sequences; hence, arginine at position 289 is indispensable for *Irf8* function) (Fig. 1F) (23, 37, 39).

To analyze the detailed morphology, we performed confocal and electron microscopy studies on DC9 cells (Fig. 2). *Irf8*-expressing DC9 cells showed elongated dendrite formation displaying a maturation phenotype upon treatment with TLR9 ligand (CpG), whereas control vector–transduced cells did not show any change in cell morphology (Fig. 2A). Electron microscopy studies of DC9 cells showed an indented nucleus and a packed cytoplasm abundantly occupied by mitochondria and rough endoplasmic reticulum. The size of the Golgi apparatus and the abundance of endoplasmic reticulum suggest a rich proteomic synthesis/activity (Fig. 2B). No major morphological changes were noticed between control cells and the *Irf8*-expressing population, whereas an increase in the size and abundance of the dendrites was seen in CpG-stimulated populations (Fig. 2B). A strict quantification of the dendrite is technically challenging because we are looking at only a cross-section; nevertheless, the CpG-stimulated *Irf8*-expressing population showed a membrane that is more convoluted than the control population, and the dendrites always appeared to be very long (>5 μm).

To study the response of DC9 cells to different TLR ligands, we treated control and *Irf8*-expressing cells with CpG and LPS (Fig. 3A, 3B). The responses of control and *Irf8*-expressing DC9 cell populations to the TLR ligands were comparable to that reported with *Irf8*$^{+/+}$ and *Irf8*$^{-/-}$ BMDCs (18, 23, 42). Selectively, only the cell population expressing *Irf8* and stimulated with CpG showed an increase in the type I IFN gene (*Ifna* and *Ifnb*) transcripts. Induction of *Il12p40* and *Il1b* genes was very high in *Irf8*-expressing cells compared with control vector–transduced cells upon stimulation. Levels of *Tnfa* transcripts were higher in CpG-stimulated *Irf8*-expressing cells, whereas the levels were comparable in LPS-stimulated populations. CD8α induction was seen only in *Irf8*-transduced cells. CD8α marker was induced more efficiently in *Irf8* expressing DC9 cells upon CpG stimulation compared to LPS treated cells, although the surface expression levels of MHCII were comparable between CpG and LPS stimulation of each cell population. To study in vivo differentiation of DC9 cells, control (Mig-control-IRES-hCD8t) and *Irf8*-expressing (Mig-*Irf8*-IRES-hCD8t) populations were introduced into mice by retro-orbital injection. Analysis

of human CD8-expressing splenic cell populations showed that only the *Irf8*-expressing population developed into CD8α$^+$ DCs and displayed very high levels of MHCII expression compared with the control vector–transduced population (Fig. 3C).

Irf8 is master regulator of classical CD8α$^+$ DC differentiation

Irf8 is essential for development of pDCs and CD8α$^+$ DCs. *Id2* and *Batf3* are also essential for development of the CD8α$^+$ DC subset. Hence, we studied the importance of each of these three transcription factors in CD8α$^+$ DC development. *Id2* and *Batf3* transcripts were at almost undetectable levels in *Irf8*$^{-/-}$ DCs compared with *Irf8*$^{+/+}$ DCs, and expression of *Irf8* in DC9 cells led to an increase in *Id2* and *Batf3* transcripts, suggesting that *Irf8* is critical for expression of *Id2* and *Batf3*. In agreement with an increase in transcript levels, we also noted an increase in *Id2* protein levels in DC9 cells expressing *Irf8* (Fig. 4A). One recent report (33) suggested that, in the absence of *Batf3*, *Batf* and *Batf2* can direct the compensatory CD8α$^+$ DC development during infection with intracellular pathogens. Cytokines IL-12 and IFN-γ are critical for compensatory CD8α$^+$ DC development. Expression analysis of members of the *Batf* family suggests that *Irf8* specifically induced *Batf3* expression and not *Batf* or *Batf2* transcripts (Fig. 4B). Thus, we examined whether induction of *Id2* and *Batf3* by *Irf8* plays a decisive role in CD8α$^+$ DC development or whether *Irf8* has a larger role, in addition to its regulation of *Id2* and *Batf3*. To understand the effect of individual gene expression and the synergistic/antagonistic effect, if any, we expressed *Irf8*, *Id2*, and *Batf3* individually and together in DC9 cells. Expression of *Id2* alone, *Batf3* alone, or *Id2* and *Batf3* together did not induce CD8α$^+$ DCs (Fig. 4C). However, when expressed with *Irf8*, *Id2* and *Batf3* showed a synergistic increase in the induction of CD8α$^+$ cells. Similarly, *Batf3* and *Id2*, when expressed with *Irf8*, showed a synergistic increase in MHCII expression upon stimulation by CpG. We observed high levels of MHCII expression in cells coexpressing *Id2* and *Irf8* without CpG stimulation, which increased further upon CpG stimulation (Supplemental Fig. 3A). Synergism between *Id2* and *Batf3* with *Irf8* was also observed in the induction of DC-activation markers CD40 and CD80 (Fig. 4D). Expression of pan DC marker CD11c was downregulated by *Id2*, and it was downregulated further by coexpression of *Batf3* and *Id2*. We observed a decrease in the levels of the pDC-specific marker SiglecH by *Batf3*. *Id2* expression alone or *Id2* and *Batf3* together downregulated SiglecH to undetectable levels. CD11c and SiglecH downregulation by *Id2* and/or *Batf3* was rescued by the expression of *Irf8* (Fig. 4E).

Batf3 *and* Id2 have a synergistic effect on Irf8-directed classical CD8α$^+$ DC–specific gene expression

We extended our study further by examining the gene expression pattern of subset-specific transcripts by semiquantitative PCR. Comparative studies between equivalent mouse and human CD8α$^+$ DC populations identified *Xcr1*, *Necl2*, and *Clec9a* as subset-specific transcripts. Expression of *Irf8* led to an increase in CD8α$^+$ DC–specific transcripts, such as *Clec9a*, *Xcr1*, *Necl2*, *Tlr3*, and *Tlr11*, and pDC-specific gene transcripts, such as *Siglech*, *Spib*, *Tlr9*, *Irf7*, and *Mgl1* (Fig. 5). In accordance with the surface marker analysis, the synergistic effect of coexpression of *Id2* and *Batf3* with *Irf8* was specific to the induction of CD8α$^+$ DC–specific transcripts, whereas no major changes were noted in pDC-specific transcripts (Fig. 5). Coexpression of *Id2* with *Irf8* led to the synergistic increase in *Batf3*;

similarly, coexpression of *Batf3* with *Irf8* led to an increase in *Id2* transcript levels. As noted by surface marker staining, we observed a decrease in Siglech transcript levels by *Id2* and *Batf3* and noted that the *Irf8*-induced levels of Siglech were reduced further by expression of *Batf3* and *Id2* (Fig. 5B). Coexpression of *Id2* and *Batf3* in wild-type bone marrow cultures suppressed the $B220^+$ pDC population, even in the presence of cells endogenous *Irf8* expression (data not shown). We observed that the cDC-specific gene zDC (*Zbtb46*) is efficiently induced by *Irf8*, suggesting that *Irf8* is upstream of zDC in the cDC developmental scheme. Further coexpression with *Id2* or *Batf3* led to a synergistic increase in zDC levels (Supplemental Fig. 3B).

A recent report (34) suggested that *Nfil3* regulates *Batf3* expression and, thus, plays a critical role in $CD8\alpha^+$ DC development. We examined whether expression of *Nfil3* alone could rescue the $CD8\alpha^+$ DC phenotype in the *Irf8*-null background. *Nfil3* expression in DC9 cells showed a modest increase in MHCII induction upon CpG treatment, although $CD8\alpha$ could not be detected. We further examined the $CD8\alpha^+$ DC–specific gene induction pattern by *Nfil3* in comparison with *Irf8* expression (Supplemental Fig. 4). We noticed a modest, yet reproducible 2-fold, increase in *Nfil3* transcript levels in the *Irf8*-expressing population. $CD8\alpha^+$ DC–specific genes, such as *Necl2*, *Xcr1*, and *Tlr3*, were induced at comparable levels by *Nfil3*, yet *Irf8* expression led to comparably higher levels of key transcription factors *Batf3* and *Id2*. The *Clec9a* gene remained undetected in *Nfil3*-expressing cells and appeared specifically upon *Irf8* expression.

Discussion

Because of the lack of readily available appropriately characterized DC cell lines and the limitation on the number of DCs available from ex vivo or in vitro cultures, key molecules that govern DC development and function have been identified using knockout mouse models; however; the molecular mechanism for the developmental program and DC function are not fully understood (4). In the present study, we demonstrated development of the Flt3-L– dependent mouse DC progenitor-like cells from $Irf8^{-/-}$ mice. DC9 cells are trapped in a progenitor-like stage and are unable to advance through further differentiation because of the absence of *Irf8*. It is noteworthy that, upon *Irf8* transduction, DC9 cells underwent growth arrest concomitant with differentiation into immature DCs. This growth arrest is not surprising, given *Irf8*'s well-documented activity to inhibit cell growth (43, 44). *Irf8* inhibits proliferation of myeloid progenitor cells through multiple pathways involving the activation of several genes that interfere with the c-Myc pathway and induction of the CDK inhibitor INK4 (43, 44). Thus, *Irf8* is a potent leukemia suppressor, capable of inhibiting proliferation of BCR/abl-transformed cells (45, 46). It was shown that *Irf8* is downregulated in some cancers (47, 48). *Irf8* separates the transcriptional program of DC development from the macrophage lineage, and it is required for the transition of macrophage–DC progenitors to common DC progenitors (49). The current study extends IRF8's growth-inhibitory activity from myeloid cells to cells of the DC lineage. There is little doubt that the absence of IRF8-mediated growth inhibition enabled DC9 cells to proliferate continuously in culture. In support of this suggestion, the Tot2 cell line, perpetually growing myeloid progenitor cells from $Irf8^{-/-}$ mice, was reported to differentiate into macrophages upon *Irf8* expression (43, 44). Clearly, the absence of *IRF8* was a critical

requirement for establishing progenitor cells, because neither DC progenitors nor myeloid progenitors could be established from wild-type mice in the current or previous studies. A novel aspect of DC9 cells is that, upon *Irf8* transduction, the cells differentiate into "immature" DCs and express transcription factors *Spib*, *Id2*, and *Batf3*, which are specific to pDCs and the CD8α$^+$ DC subtype. Most significantly, *Irf8* conferred the ability to respond to TLR ligands, resulting in increased expression of MHCII and CD8α on the surface, and induced type I IFNs and IL-12, the cytokines that define pDCs and CD8α$^+$ DCs, respectively, in addition to other inflammatory cytokines. As reported in our earlier studies (18, 23, 39), type I IFNs (*Ifna* and *Ifnb*) and *Il12p40* were induced in cells expressing *Irf8* and remained at very low levels in control cells, thus further confirming observations that *Irf8* is required for the expression of these cytokines in DCs. *Tnfa* is induced at comparable levels in LPS-stimulated populations, whereas levels for CpG-treated populations were higher in the *Irf8*-expressing cells. This observation further strengthens our previous report (42) suggesting that mechanisms of NF-κB activation by CpG and LPS are different and that *Irf8* plays a critical role in TLR9 signaling. *Irf8* expression in DC9 cells showed that it led to the induction of pDC- and CD8α$^+$ DC–specific transcripts, as well as induced effector cytokines. Together, in light of the availability of relatively large numbers of a homogeneous cell population, DC9 cells offer a novel experimental model suitable for studying molecular and biochemical aspects of DC differentiation, which is otherwise difficult to achieve with ex vivo or in vitro manipulation of cells. Furthermore, differentiation of DC9 cells into immature DCs and their ability to function as mature DCs upon TLR stimulation, to produce type I IFNs and effector cytokines, offer additional useful qualities not present in other DC lines available in the field, most of which originated from tumors (50–52).

Our previous reports (18, 23, 37, 38, 53) showed conclusively that *Irf8* is required for development of pDCs and CD8α$^+$ DCs. *Irf8* not only regulates the differentiation of DCs, it also plays a critical role in the production of cytokines of innate immune effect; furthermore, it is important in efficient Ag presentation, leading to decisions about the types of adaptive immune responses (18, 38, 39, 54). A recent study (26) suggested that E2.2 is required for the development of pDCs and, indeed, it directly controls *Irf8* expression. *E2.2* levels remained unaffected in control and *Irf8*-expressing populations, implying that *Irf8* itself does not regulate E2.2 expression. Nevertheless, a subset of pDC-specific genes was not expressed in DC9 cells but was induced following *Irf8* transduction, suggesting that IRF8 and E2.2 may cooperate to direct the pDC-specific developmental programs. The universality of CD8α$^+$ DCs was confirmed recently with the identification of a human equivalent of the CD8α$^+$ subset (9–13). These studies led to the identification of a subgroup of genes that are specifically expressed in the CD8α$^+$ DC subset. *Irf8*, *Id2*, and *Batf3* are the three transcription factors that are essential for the development of CD8α$^+$ DCs (18, 23, 27, 53, 55, 56). In a recent study (33), an alternative CD8α$^+$ DC developmental program was demonstrated in which the absence of *Batf3* was compensated for by *Batf* or *Batf2*, although the detailed transcriptional profiling of alternative CD8α$^+$ DCs remains to be investigated. In our model, expression of *Irf8* specifically induced *Batf3* gene transcripts, and not the *Batf* or *Batf2* transcripts; thus, our model represents the development of *Batf3*-dependent classical CD8α$^+$ DCs. We showed that *Id2* and *Batf3* were expressed at very low levels in

Irf8$^{-/-}$ BMDCs and DC9 cells, and these genes were induced after *Irf8* transduction. These observations imply that *Id2* and *Batf3* are downstream targets of *Irf8* and are activated directly or indirectly by *Irf8*. *Batf3* and *Id2* are essential for classical CD8α$^+$ DC development, and our results imply that expression of *Batf3* and *Id2* was not sufficient to regulate requisite developmental programs. When expressed along with *Irf8*, *Id2* and *Batf3* have a synergistic effect on specific gene subsets, leading to classical CD8α$^+$ DCs. Our results are also supported by the phenotypes of mice lacking *Irf8*, *Id2*, and *Batf3*, which display lack of CD103$^+$CD11b$^-$ cDCs that are similar to CD8α$^+$ DCs (31, 32, 57). As reported earlier, *Id2* (or *Id3*) expression in progenitor cells inhibits pDC development and directs DC development toward conventional DCs (28). In our experiments with DC9 cells and bone marrow cultures, we observed that *Id2* along with *Batf3* decreased pDC-specific gene expression, leading to downregulation of pDC development. Thus, *Id2* and *Batf3* play a dual role in DC differentiation; they arrest pDC development by inhibiting the E2.2-directed pDC developmental program, and they increase the CD8α$^+$ DC–specific gene transcription in synergism with *Irf8*. In agreement with the antagonism by factors specific for CD8α$^+$ DCs, we also observed that transduction of *Batf3* and *Id2* inhibited expression of the pDC-specific marker SiglecH. However, other pDC genes were not affected by *Id2* or *Batf3* as in current study we ectopically coexpressed *Irf8* in DC9 cells along with *Id2* and *Batf3* under an exogenous promoter, thus circumventing the requirement of *E2.2* for *Irf8* gene expression. Furthermore, under the retroviral promoter, *Irf8* transcript levels were immune to functional inhibition of *E2.2* by *Id2*. Our results indicate that IRF8 itself does not dictate the developmental choice between pDCs and CD8α$^+$ DCs; the subset decision is more heavily dependent on the downstream factors *Id2* and *Batf3*. One can envisage that, during development in vivo, the timing and the levels of *Irf8* expression would affect the relative levels of *E2.2* vis-a-vis *Id2/Batf3*, which would favor developmental pathways either for pDCs or CD8α$^+$ DCs. We consider that DC9 cells maintain the dual properties, because the timing and levels of *Irf8* expression are different from those in vivo. Transduction of *Nfil3* activated a limited subset of CD8α$^+$ DC genes that is probably activated by *Batf3* (and *Irf8*). In contrast, *Irf8* alone activated a broader set of CD8α$^+$ DC genes, suggesting that *Nfil3* is involved in activating a restricted pathway of CD8α$^+$ DC development that aligns with *Batf3*. Further indepth experiments with different knockout mouse models would help to decipher the specific contribution of *Id2*, *Nfil3*, and *Batf3* in *Irf8*-directed CD8α$^+$ DC development.

In summary, analysis of DC9 cells, a newly established DC progenitor-like cell line, demonstrates that *Irf8* activates the developmental pathways for pDCs and CD8α$^+$ DCs by the timely expression of transcription factors that define two DC subsets. *Irf8* upregulates *Id2* and *Batf3* expression. *Id2* and *Batf3* expression are not sufficient for directing CD8α$^+$ DC development; however, when expressed along with *Irf8* they have a synergistic effect in directing DC development toward the CD8α$^+$ DC lineage. *Irf8* also facilitates functional maturation of these DCs by activating TLR-signaling pathways that allow production of DC subtype– specific signature cytokines: type I IFNs and IL-12. Together, our data demonstrate that *Irf8* is a master regulator of classical CD8α$^+$ DC development.

Supplementary Material

Refer to Web version on PubMed Central for supplementary material.

Acknowledgments

We thank Prof. Ben-Zion Levi (Technion, Haifa, Israel) and Drs. Robin Mukhopadhyaya and Ajit Chande (Advanced Centre for Treatment, Research and Education in Cancer, Navi Mumbai, Maharashtra, India) for helpful discussions. We also thank Dr. Robin Mukhopadhyaya for careful reading of the manuscript.

This work was supported by the National Institute of Immunology Core Fund. P.T. is a Ramalingaswami fellow, Department of Biotechnology, "Government of India" at National Institute of Immunology. H.J. and R.V. are supported by a fellowship from the Council for Scientific and Industrial Research, Government of India. M.K. is supported by a contingency grant of the Ramalingaswami Fellowship awarded to P.T.

Abbreviations used in this article

BMDC	bone marrow–derived dendritic cell
cDC	conventional dendritic cell
DC	dendritic cell
IRES	internal ribosomal entry site
MHCII	MHC class II
MSCV	Murine stem cell virus
pDC	plasmacytoid DC

References

1. Steinman RM, Idoyaga J. Features of the dendritic cell lineage. Immunol. Rev. 2010; 234:5–17. [PubMed: 20193008]
2. Belz GT, Nutt SL. Transcriptional programming of the dendritic cell network. Nat. Rev. Immunol. 2012; 12:101–113. [PubMed: 22273772]
3. Shortman K, Liu Y-J. Mouse and human dendritic cell subtypes. Nat. Rev. Immunol. 2002; 2:151–161. [PubMed: 11913066]
4. Geissmann F, Manz MG, Jung S, Sieweke MH, Merad M, Ley K. Development of monocytes, macrophages, and dendritic cells. Science. 2010; 327:656–661. [PubMed: 20133564]
5. Robbins SH, Walzer T, Dembélé D, Thibault C, Defays A, Bessou G, Xu H, Vivier E, Sellars M, Pierre P, et al. Novel insights into the relationships between dendritic cell subsets in human and mouse revealed by genome-wide expression profiling. Genome Biol. 2008; 9:R17. [PubMed: 18218067]
6. Asselin-Paturel C, Trinchieri G. Production of type I interferons: plasmacytoid dendritic cells and beyond. J. Exp. Med. 2005; 202:461–465. [PubMed: 16103406]
7. Villadangos JA, Young L. Antigen-presentation properties of plasmacytoid dendritic cells. Immunity. 2008; 29:352–361. [PubMed: 18799143]
8. Siegal FP, Kadowaki N, Shodell M, Fitzgerald-Bocarsly PA, Shah K, Ho S, Antonenko S, Liu Y-J. The nature of the principal type 1 interferon-producing cells in human blood. Science. 1999; 284:1835–1837. [PubMed: 10364556]
9. Jongbloed SL, Kassianos AJ, McDonald KJ, Clark GJ, Ju X, Angel CE, Chen CJ, Dunbar PR, Wadley RB, Jeet V, et al. Human $CD141^{+}$ $(BDCA\text{-}3)^{+}$ dendritic cells (DCs) represent a unique myeloid DC subset that cross-presents necrotic cell antigens. J. Exp. Med. 2010; 207:1247–1260. [PubMed: 20479116]

10. Poulin LF, Salio M, Griessinger E, Anjos-Afonso F, Craciun L, Chen J-L, Keller AM, Joffre O, Zelenay S, Nye E, et al. Characterization of human DNGR-1^{+} BDCA3^{+} leukocytes as putative equivalents of mouse CD8α^{+} dendritic cells. J. Exp. Med. 2010; 207:1261–1271. [PubMed: 20479117]
11. Crozat K, Guiton R, Contreras V, Feuillet V, Dutertre C-A, Ventre E, Vu Manh T-P, Baranek T, Storset AK, Marvel J, et al. The XC chemokine receptor 1 is a conserved selective marker of mammalian cells homologous to mouse CD8α^{+} dendritic cells. J. Exp. Med. 2010; 207:1283–1292. [PubMed: 20479118]
12. Bachem A, Güttler S, Hartung E, Ebstein F, Schaefer M, Tannert A, Salama A, Movassaghi K, Opitz C, Mages HW, et al. Superior antigen cross-presentation and XCR1 expression define human CD11c^{+}CD141^{+} cells as homologues of mouse CD8^{+} dendritic cells. J. Exp. Med. 2010; 207:1273–1281. [PubMed: 20479115]
13. Villadangos JA, Shortman K. Found in translation: the human equivalent of mouse CD8^{+} dendritic cells. J. Exp. Med. 2010; 207:1131–1134. [PubMed: 20513744]
14. Merad M, Ginhoux F. Dendritic cell genealogy: a new stem or just another branch? Nat. Immunol. 2007; 8:1199–1201. [PubMed: 17952047]
15. Onai N, Obata-Onai A, Schmid MA, Ohteki T, Jarrossay D, Manz MG. Identification of clonogenic common Flt3^{+}M-CSFR^{+} plasmacytoid and conventional dendritic cell progenitors in mouse bone marrow. Nat. Immunol. 2007; 8:1207–1216. [PubMed: 17922016]
16. Naik SH, Sathe P, Park H-Y, Metcalf D, Proietto AI, Dakic A, Carotta S, O'Keeffe M, Bahlo M, Papenfuss A, et al. Development of plasmacytoid and conventional dendritic cell subtypes from single precursor cells derived in vitro and in vivo. Nat. Immunol. 2007; 8:1217–1226. [PubMed: 17922015]
17. Gilliet M, Boonstra A, Paturel C, Antonenko S, Xu X-L, Trinchieri G, O'Garra A, Liu Y-J. The development of murine plasmacytoid dendritic cell precursors is differentially regulated by FLT3-ligand and granulocyte/macrophage colony-stimulating factor. J. Exp. Med. 2002; 195:953–958. [PubMed: 11927638]
18. Tamura T, Tailor P, Yamaoka K, Kong HJ, Tsujimura H, O'Shea JJ, Singh H, Ozato K. IFN regulatory factor-4 and -8 govern dendritic cell subset development and their functional diversity. J. Immunol. 2005; 174:2573–2581. [PubMed: 15728463]
19. Fancke B, Suter M, Hochrein H, O'Keeffe M. M-CSF: a novel plasmacytoid and conventional dendritic cell poietin. Blood. 2008; 111:150–159. [PubMed: 17916748]
20. Esashi E, Wang Y-H, Perng O, Qin X-F, Liu Y-J, Watowich SS. The signal transducer STAT5 inhibits plasmacytoid dendritic cell development by suppressing transcription factor IRF8. Immunity. 2008; 28:509–520. [PubMed: 18342552]
21. Schiavoni G, Mattei F, Sestili P, Borghi P, Venditti M, Morse HC III, Belardelli F, Gabriele L. ICSBP is essential for the development of mouse type I interferon-producing cells and for the generation and activation of CD8α(+) dendritic cells. J. Exp. Med. 2002; 196:1415–1425. [PubMed: 12461077]
22. Suzuki S, Honma K, Matsuyama T, Suzuki K, Toriyama K, Akitoyo I, Yamamoto K, Suematsu T, Nakamura M, Yui K, Kumatori A. Critical roles of interferon regulatory factor 4 in CD11b^{high}CD8α^{-} dendritic cell development. Proc. Natl. Acad. Sci. USA. 2004; 101:8981–8986. [PubMed: 15184678]
23. Tailor P, Tamura T, Morse HC III, Ozato K. The BXH2 mutation in IRF8 differentially impairs dendritic cell subset development in the mouse. Blood. 2008; 111:1942–1945. [PubMed: 18055870]
24. Honda K, Mizutani T, Taniguchi T. Negative regulation of IFN-α/β signaling by IFN regulatory factor 2 for homeostatic development of dendritic cells. Proc. Natl. Acad. Sci. USA. 2004; 101:2416–2421. [PubMed: 14983024]
25. Gabriele L, Fragale A, Borghi P, Sestili P, Stellacci E, Venditti M, Schiavoni G, Sanchez M, Belardelli F, Battistini A. IRF-1 deficiency skews the differentiation of dendritic cells toward plasmacytoid and tolerogenic features. J. Leukoc. Biol. 2006; 80:1500–1511. [PubMed: 16966383]

26. Cisse B, Caton ML, Lehner M, Maeda T, Scheu S, Locksley R, Holmberg D, Zweier C, den Hollander NS, Kant SG, et al. Transcription factor E2-2 is an essential and specific regulator of plasmacytoid dendritic cell development. Cell. 2008; 135:37–48. [PubMed: 18854153]
27. Hacker C, Kirsch RD, Ju X-S, Hieronymus T, Gust TC, Kuhl C, Jorgas T, Kurz SM, Rose-John S, Yokota Y, Zenke M. Transcriptional profiling identifies Id2 function in dendritic cell development. Nat. Immunol. 2003; 4:380–386. [PubMed: 12598895]
28. Spits H, Couwenberg F, Bakker AQ, Weijer K, Uittenbogaart CH. Id2 and Id3 inhibit development of CD34($^{+}$) stem cells into predendritic cell (pre-DC)2 but not into pre-DC1. Evidence for a lymphoid origin of pre-DC2. J. Exp. Med. 2000; 192:1775–1784. [PubMed: 11120774]
29. Schotte R, Nagasawa M, Weijer K, Spits H, Blom B. The ETS transcription factor Spi-B is required for human plasmacytoid dendritic cell development. J. Exp. Med. 2004; 200:1503–1509. [PubMed: 15583020]
30. Allman D, Dalod M, Asselin-Paturel C, Delale T, Robbins SH, Trinchieri G, Biron CA, Kastner P, Chan S. Ikaros is required for plasmacytoid dendritic cell differentiation. Blood. 2006; 108:4025–4034. [PubMed: 16912230]
31. Ginhoux F, Liu K, Helft J, Bogunovic M, Greter M, Hashimoto D, Price J, Yin N, Bromberg J, Lira SA, et al. The origin and development of nonlymphoid tissue CD103^{+} DCs. J. Exp. Med. 2009; 206:3115–3130. [PubMed: 20008528]
32. Edelson BT, Kc W, Juang R, Kohyama M, Benoit LA, Klekotka PA, Moon C, Albring JC, Ise W, Michael DG, et al. Peripheral CD103^{+} dendritic cells form a unified subset developmentally related to CD8α^{+} conventional dendritic cells. J. Exp. Med. 2010; 207:823–836. [PubMed: 20351058]
33. Tussiwand R, Lee W-L, Murphy TL, Mashayekhi M, Wumesh KC, Albring JC, Satpathy AT, Rotondo JA, Edelson BT, Kretzer NM, et al. Compensatory dendritic cell development mediated by BATF-IRF interactions. Nature. 2012; 490:502–507. [PubMed: 22992524]
34. Kashiwada M, Pham NL, Pewe LL, Harty JT, Rothman PB. NFIL3/E4BP4 is a key transcription factor for CD8α^{+} dendritic cell development. Blood. 2011; 117:6193–6197. [PubMed: 21474667]
35. Satpathy AT, Kc W, Albring JC, Edelson BT, Kretzer NM, Bhattacharya D, Murphy TL, Murphy KM. Zbtb46 expression distinguishes classical dendritic cells and their committed progenitors from other immune lineages. J. Exp. Med. 2012; 209:1135–1152. [PubMed: 22615127]
36. Meredith MM, Liu K, Kamphorst AO, Idoyaga J, Yamane A, Guermonprez P, Rihn S, Yao K-H, Silva IT, Oliveira TY, et al. Zinc finger transcription factor zDC is a negative regulator required to prevent activation of classical dendritic cells in the steady state. J. Exp. Med. 2012; 209:1583–1593. [PubMed: 22851594]
37. Tsujimura H, Tamura T, Gongora C, Aliberti J, Reis e Sousa C, Sher A, Ozato K. ICSBP/IRF-8 retrovirus transduction rescues dendritic cell development in vitro. Blood. 2003; 101:961–969. [PubMed: 12393459]
38. Tsujimura H, Tamura T, Ozato K. Cutting edge: IFN consensus sequence binding protein/IFN regulatory factor 8 drives the development of type I IFN-producing plasmacytoid dendritic cells. J. Immunol. 2003; 170:1131–1135. [PubMed: 12538667]
39. Tailor P, Tamura T, Kong HJ, Kubota T, Kubota M, Borghi P, Gabriele L, Ozato K. The feedback phase of type I interferon induction in dendritic cells requires interferon regulatory factor 8. Immunity. 2007; 27:228–239. [PubMed: 17702615]
40. Tamura T, Thotakura P, Tanaka TS, Ko MSH, Ozato K. Identification of target genes and a unique cis element regulated by IRF-8 in developing macrophages. Blood. 2005; 106:1938–1947. [PubMed: 15947094]
41. Curry JM, Eubank TD, Roberts RD, Wang Y, Pore N, Maity A, Marsh CB. M-CSF signals through the MAPK/ERK pathway via Sp1 to induce VEGF production and induces angiogenesis in vivo. PLoS ONE. 2008; 3:e3405. [PubMed: 18852899]
42. Tsujimura H, Tamura T, Kong HJ, Nishiyama A, Ishii KJ, Klinman DM, Ozato K. Toll-like receptor 9 signaling activates NF-kappaB through IFN regulatory factor-8/IFN consensus sequence binding protein in dendritic cells. J. Immunol. 2004; 172:6820–6827. [PubMed: 15153500]

43. Tamura T, Nagamura-Inoue T, Shmeltzer Z, Kuwata T, Ozato K. ICSBP directs bipotential myeloid progenitor cells to differentiate into mature macrophages. Immunity. 2000; 13:155–165. [PubMed: 10981959]
44. Schmidt M, Bies J, Tamura T, Ozato K, Wolff L. The interferon regulatory factor ICSBP/IRF-8 in combination with PU.1 up-regulates expression of tumor suppressor p15(Ink4b) in murine myeloid cells. Blood. 2004; 103:4142–4149. [PubMed: 14976051]
45. Tamura T, Kong HJ, Tunyaplin C, Tsujimura H, Calame K, Ozato K. ICSBP/IRF-8 inhibits mitogenic activity of p210 Bcr/Abl in differentiating myeloid progenitor cells. Blood. 2003; 102:4547–4554. [PubMed: 12933588]
46. Nardi V, Naveiras O, Azam M, Daley GQ. ICSBP-mediated immune protection against BCR-ABL-induced leukemia requires the CCL6 and CCL9 chemokines. Blood. 2009; 113:3813–3820. [PubMed: 19171873]
47. Hao SX, Ren R. Expression of interferon consensus sequence binding protein (ICSBP) is downregulated in Bcr-Abl-induced murine chronic myelogenous leukemia-like disease, and forced coexpression of ICSBP inhibits Bcr-Abl-induced myeloproliferative disorder. Mol. Cell. Biol. 2000; 20:1149–1161. [PubMed: 10648600]
48. Yang D, Thangaraju M, Greeneltch K, Browning DD, Schoenlein PV, Tamura T, Ozato K, Ganapathy V, Abrams SI, Liu K. Repression of IFN regulatory factor 8 by DNA methylation is a molecular determinant of apoptotic resistance and metastatic phenotype in metastatic tumor cells. Cancer Res. 2007; 67:3301–3309. [PubMed: 17409439]
49. Schönheit J, Kuhl C, Gebhardt ML, Klett FF, Riemke P, Scheller M, Huang G, Naumann R, Leutz A, Stocking C, et al. PU.1 level-directed chromatin structure remodeling at the Irf8 gene drives dendritic cell commitment. Cell Rep. 2013; 3:1617–1628. [PubMed: 23623495]
50. Shen Z, Reznikoff G, Dranoff G, Rock KL. Cloned dendritic cells can present exogenous antigens on both MHC class I and class II molecules. J. Immunol. 1997; 158:2723–2730. [PubMed: 9058806]
51. Maeda T, Murata K, Fukushima T, Sugahara K, Tsuruda K, Anami M, Onimaru Y, Tsukasaki K, Tomonaga M, Moriuchi R, et al. A novel plasmacytoid dendritic cell line, CAL-1, established from a patient with blastic natural killer cell lymphoma. Int. J. Hematol. 2005; 81:148–154. [PubMed: 15765784]
52. Kammertoens T, Willebrand R, Erdmann B, Li L, Li Y, Engels B, Uckert W, Blankenstein T. CY15, a malignant histiocytic tumor that is phenotypically similar to immature dendritic cells. Cancer Res. 2005; 65:2560–2564. [PubMed: 15805249]
53. Aliberti J, Schulz O, Pennington DJ, Tsujimura H, Reis e Sousa C, Ozato K, Sher A. Essential role for ICSBP in the in vivo development of murine CD8α$^+$ dendritic cells. Blood. 2003; 101:305–310. [PubMed: 12393690]
54. Turcotte K, Gauthier S, Malo D, Tam M, Stevenson MM, Gros P. Icsbp1/IRF-8 is required for innate and adaptive immune responses against intracellular pathogens. J. Immunol. 2007; 179:2467–2476. [PubMed: 17675508]
55. Hildner K, Edelson BT, Purtha WE, Diamond M, Matsushita H, Kohyama M, Calderon B, Schraml BU, Unanue ER, Diamond MS, et al. Batf3 deficiency reveals a critical role for CD8α$^+$ dendritic cells in cytotoxic T cell immunity. Science. 2008; 322:1097–1100. [PubMed: 19008445]
56. Jackson JT, Hu Y, Liu R, Masson F, D'Amico A, Carotta S, Xin A, Camilleri MJ, Mount AM, Kallies A, et al. Id2 expression delineates differential checkpoints in the genetic program of CD8α$^+$ and CD103$^+$ dendritic cell lineages. EMBO J. 2011; 30:2690–2704. [PubMed: 21587207]
57. Scott CL, Aumeunier AM, Mowat AM. Intestinal CD103$^+$ dendritic cells: master regulators of tolerance? Trends Immunol. 2011; 32:412–419. [PubMed: 21816673]

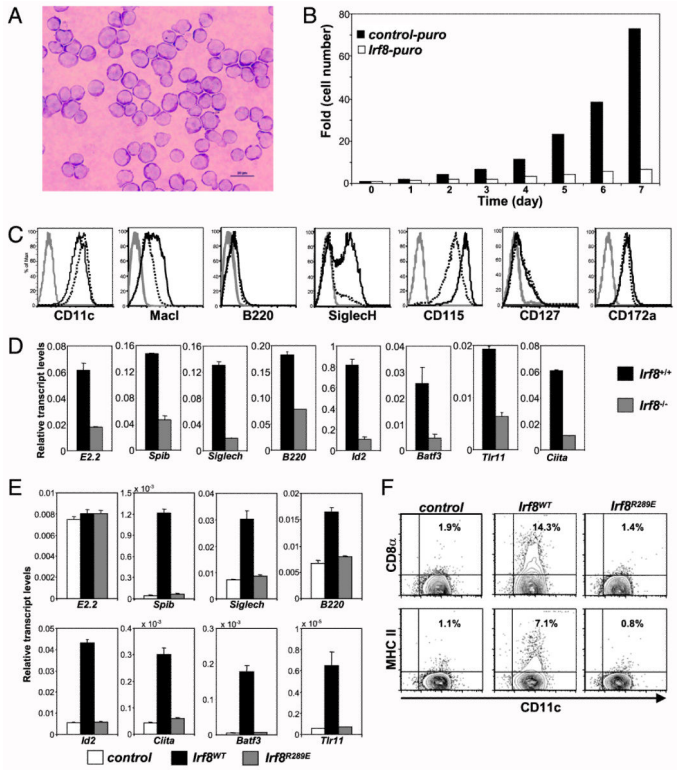

FIGURE 1.

Characterization of DC9 cell line. (**A**) Cytospin preparations of DC9 cells were subjected to Giemsa staining and observed using an oil-immersion lens. Scale bar, 20 μm. (**B**) Control vector–transduced cells grow uninhibitedly, whereas *Irf8*-expressing DC9 cells show a growth arrest. (**C**) DC9 cells were transduced with MSCV-control-puro and MSCV-*Irf8*-puro retroviruses, cells were selected for 48 h with puromycin, and populations were examined by flow cytometry. Control cells (dotted line) and *Irf8*-expressing cells (solid line) with respective marker are shown in individual graphs; isotype-control Ab staining is represented by the gray line. Data are a representation of three independent experiments. (**D**) pDC- and CD8α$^+$ DC–specific transcript levels were examined from *Irf8*$^{+/+}$ and *Irf8*$^{-/-}$ mice BMDC cultures. Data are representative of at least two independent experiments. (**E**) pDC- and CD8α$^+$ DC–specific transcript levels were examined in DC9 cells transduced with retroviruses MSCV-control-puro, MSCV-*Irf8* (*Irf8*^{WT})-puro, and R289E mutant MSCV-*Irf8* (*Irf8*^{R289E})-puro and selected for 48 h with puromycin. pDC- and CD8α$^+$ DC–specific transcript levels were increased only in the *Irf8*^{WT}-expressing population, whereas levels in control and *Irf8*^{R289E}-expressing cells remained at very low levels. Data are representative of three independent experiments. (**F**) DC9 cells were transduced with control, *Irf8*^{WT}, or *Irf8*^{R289E} retroviruses and selected for 48 h with puromycin. Selected populations were stimulated with CpG for 24 h, and the induction of CD8α or MHCII marker was studied by flow cytometry. Data are representative of three independent experiments.

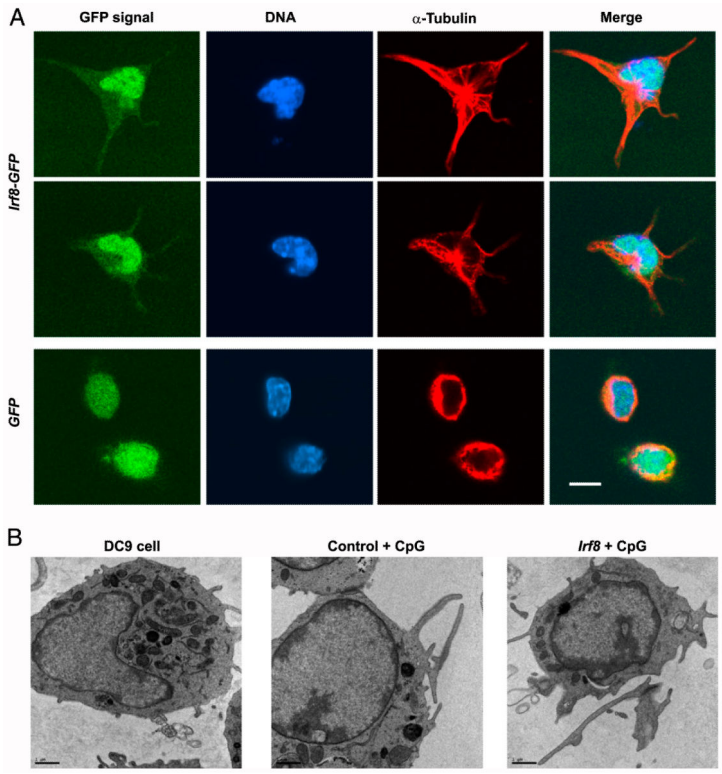

FIGURE 2.

Irf8 induces differentiation in DC9 cells. (**A**) Long dendrites are detected in DC9 cells following a 24-h treatment with TLR9 ligand (CpG) only in *Irf8-GFP*–transduced cells (*top* and *middle rows*) but not in GFP only–transduced cells (*bottom row*). *Irf8-GFP* is localized to the nucleus, whereas GFP alone is distributed in both the nucleus and the cytoplasm. α-Tubulin (red) stains the cytoplasm and dendrites. Scale bar, 8 μm. (**B**) Electron microscopy studies were performed on glutaraldehydefixed samples. DC9 parent cells showed an abundance of mitochondria and rough endoplasmic reticulum. DC9 cells were transduced with MSCV-control-puro or MSCV-*Irf8*-puro retroviruses and selected with puromycin for 48 h. Selected populations were treated with CpG for 24 h. *Irf8*-expressing DC9 cells showed comparatively longer dendrites. Scale bar, 1 μm.

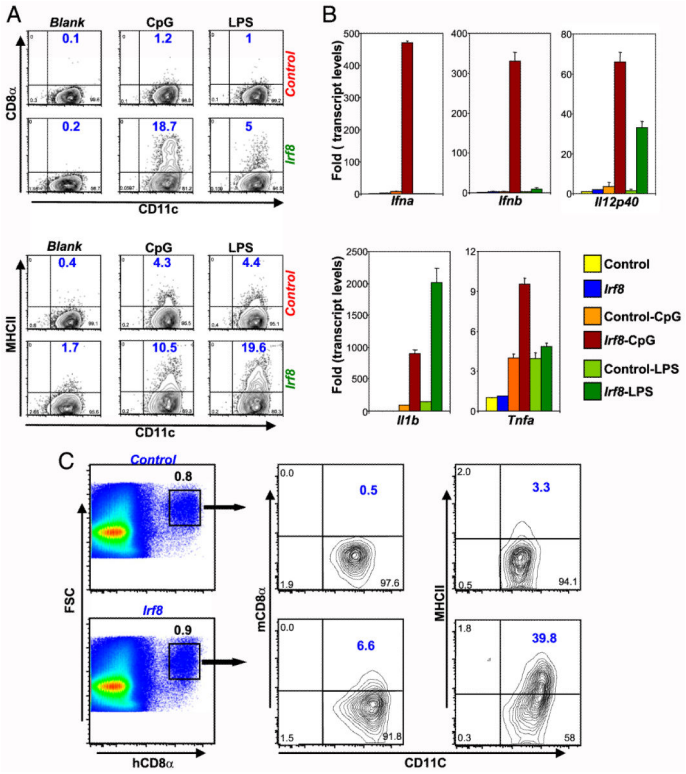

FIGURE 3.

Response of DC9 cells to various TLR ligands and in vivo study. (**A**) DC9 cells were transduced with MSCV-control-puro or MSCV-*Irf8*-puro retrovirus, and cells were selected for 48 h with puromycin. Surface expression of CD8α and MHCII markers was studied on puromycin-selected populations stimulated with CpG and LPS for 24 h or left unstimulated (Blank). Data are representative of two independent experiments. (**B**) DC9 cells were transduced with control or *Irf8* retrovirus and selected for 48 h with puromycin. Cytokine gene induction was studied by real-time PCR on selected populations stimulated with CpG and LPS for 6 h. Data are representative of three independent experiments. (**C**) DC9 cells were transduced with retrovirus Mig-control-IRES-hCD8t or Mig-*Irf8*-IRES-hCD8t, and cells were introduced into C57BL/6 mice by retro-orbital injection. Analysis of splenic human $CD8^+$ cells showed that CD8α and MHCII markers were detected on the *Irf8*-expressing population. Data are representative of two independent experiments.

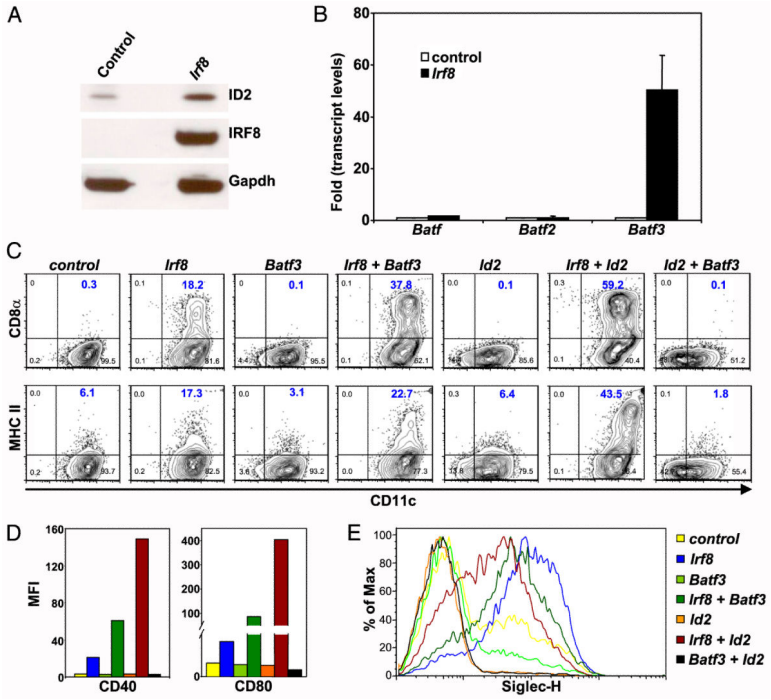

FIGURE 4.

Understanding the role of transcription factors *Irf8*, *Batf3*, and *Id2* in CD8α$^+$ DC development. (**A**) DC9 cells were transduced with Mig-control-IRES-hCD8t or Mig-*Irf8*-IRES-hCD8t retrovirus. At 72 h posttransduction, cells were purified using anti-human CD8 MicroBeads, and the *Id2* levels were compared by Western blot analysis. (**B**) DC9 cells were transduced with MSCV-control-puro or MSCV-*Irf8*-puro retrovirus, and 48-h puromycin–selected populations were analyzed for the expression of Batf family members (*Batf*, *Batf2*, and *Batf3*). (**C**) DC9 cells were transduced with retrovirus expressing *Irf8*, *Batf3*, or *Id2* individually and coexpressed with each other and selected for 48 h with puromycin. Selected populations were treated with CpG (1826; 1 μg/ml) for 24 h and analyzed by flow cytometry. Expression of *Id2* or *Batf3* alone or coexpressed together did not induce CD8α surface marker. When coexpressed with *Irf8*, *Id2* or *Batf3* showed a synergistic effect on the expression of surface markers CD8α and MHCII. Data are representative of three independent experiments. (**D**) DC9 cells were transduced with retroviruses expressing *Irf8*, *Batf3*, or *Id2* individually and coexpressed with each other and selected for 48 h with puromycin. Selected populations were treated with CpG (1826; 1 μg/ml) for 24 h and analyzed by flow cytometry. DC maturation markers CD40 and CD80 also showed a synergistic increase when *Id2* or *Batf3* was coexpressed with *Irf8*. Data are representative of three independent experiments. (*E*) DC9 cells were transduced with retroviruses expressing transcription factors and selected for 48 h with puromycin. SiglecH, pDC-specific surface marker was downregulated by *Id2* and *Batf3* alone or by their coexpression. Expression of *Irf8* rescues downregulation by *Id2* and *Batf3* and increases SiglecH on the cell surface. Data are representative of three independent experiments.

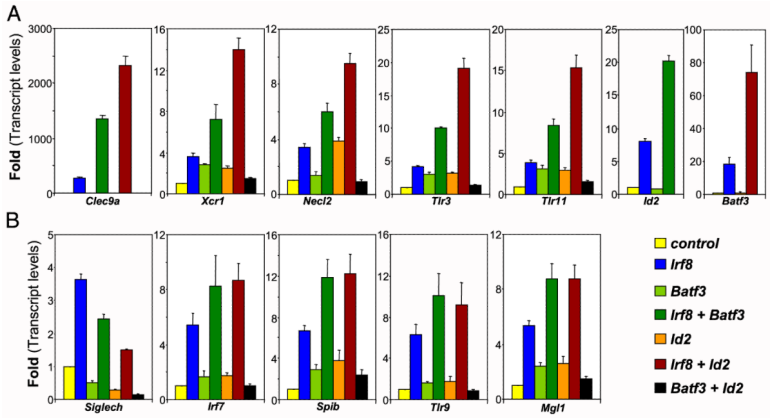

FIGURE 5.

Expression of *Batf3* and *Id2* with *Irf8* shows a synergistic activity in CD8α$^+$ DC–specific gene expression. DC9 cells were transduced with retroviruses expressing transcription factors. CD8α$^+$ DC– and pDC-specific gene-expression levels were measured by real-time PCR after a 48-h selection by puromycin. Data are representative of three independent experiments. (**A**) Expression of *Id2* or *Batf3* alone or together did not induce CD8α-specific gene expression. Coexpression of *Id2* or *Batf3* with *Irf8* led to a synergistic increase in CD8α$^+$ DC–specific gene expression. (**B**) Synergistic effect of *Id2* or *Batf3* expression with *Irf8* did not extend to pDC-specific gene expression.